

A Fast Time-domain Current Harmonic extraction Algorithm for Power Quality Improvement using Three-phase Active Power Filter

Muhammed Kashif¹, M. J. Hossain², Edstan Fernandez¹, Seyedfoad Taghizadeh¹, Vivek Sharma¹, S. M. Nawazish Ali¹, Usama Bin Irshad¹

¹School of Engineering, Macquarie University, Sydney, Australia

²School of Electrical and Data Engineering University of Technology Sydney, Australia (e-mail: jahangir.hossain@uts.edu.au)

Corresponding author: Muhammad Kashif (e-mail: muhammed.kashif@hdr.mq.edu.au).

ABSTRACT Harmonic current estimation is the key aspect of Active Power Filter (APF) control algorithms to generate a reference current for harmonic compensation. This paper proposes a novel structure for harmonic current estimation scheme based on Trigonometric Orthogonal Principle (TOP) and Self Tuning Filter (STF). The key advantages of the proposed method are its simplicity, low computational burden and faster execution time in comparison to the conventional harmonic current estimation approaches. The TOP method provides a simple and fast approach to extract the reference current, while STF provides a simplified structure to generate the required synchronization signal that eliminates the need of a Phase Locked Loop (PLL) algorithm for synchronization. As a result, it exhibits less complexity in implementation and less consumption of microcontroller's resources; thus, the proposed method can be implemented using a low-cost microcontroller. It is shown in the paper that the proposed method provides 10 times gain in processing speed as compared to the conventional DQ method. The proposed approach is analyzed in detail, and its effectiveness and superior performance are verified using simulation and experimental results.

INDEX TERMS Power Quality, APF, Harmonics, PLL, STF

I. INTRODUCTION

ADVANCEMENTS of power electronics have significantly increased the use of power converters in domestic, commercial and industrial applications for efficient energy utilization. However, it pollutes the power system with harmonics by drawing non-sinusoidal current and reactive power from the source. This non-linear behavior causes significant power losses, which not only degrade the efficiency and performance of the power system but also introduce other problems like overheating of equipment, malfunctioning of sensitive devices and a resonance problem [1]–[4]. Active power filters (APF) are being developed as a best solution to perform harmonics and reactive-power compensation in power systems [5], [6]. Different structures and topologies using passive and active power filters have been proposed in the literature, but shunt APF (SAPF) is considered the most effective tool for harmonic mitigation and addressing other power-quality issues [7]–[10].

The control structure of a three-phase SAPF as shown in

Fig. 1 generates the estimated reference current that must be generated by the power filter to mitigate harmonics and reactive power in order to get a distortion-free source current and unity power factor. The control strategy consists of three main subsystems: reference-current estimation, Inner current control (switching) and outer DC-side voltage control. Among these subsystems, the current-harmonics generation algorithm is considered to be most critical [11]–[14]. As reference-current extraction is the first algorithm in APF control, fast and accurate current-harmonics extraction is of prime importance for the effective performance of the current control loop [15], [16]. The processing of the accurate reference signal enables SAPF to perform the harmonic and reactive-power compensation effectively. It may be noted that the reference current extraction is independent to the topologies (two level, multi-level) employed [17].

Initially, analog filters such as a band-pass filter and a low-pass filter have been used for current-harmonic extraction, but the output of these filters is not precise because they

introduce phase and magnitude errors [18]. Nowadays, the harmonic-current extraction is generally achieved in one of two domains, either in the time domain or in the frequency domain. Frequency-domain methods are based on the Discrete Fourier transform (DFT) or its upgraded form the Fast Fourier transform (FFT) [19], [20]. Though these methods are accurate, the delay they bring into the system make them unfeasible for fluctuating loads. Besides, their disadvantage of slow response and spectral leakage are also not negligible. In addition, Fourier-based harmonic-extraction methods are more complicated in implementation. It requires careful consideration of the anti-aliasing filter, large memory requirements and computation power, careful application of a windowing function, and proper synchronization between fundamental frequency and sampling [21]. Time-domain methods are preferable to frequency-domain methods because of their simple and faster implementation [13]. Time-domain based approach, like Instantaneous Reactive Power Theory (IRPT) [17], [22] and Synchronous Reference Frame (SRF) [13], [23], [24], are still prevalent method despite introduction of novel approaches for reference-current generation. These well-tested methods are simple in implementation, reduce controller complexity and are suitable for practical implementation. Despite their simpler implementation and fast response, they requires a synchronization reference-phase signal, usually obtained from a PLL. PLL-based methods involve a comprehensive implementation; if the source voltage is distorted or unbalanced, the PLL requires additional filters to tackle the distortion, which increases the implementation complexity [25], [26]. This has a direct impact on the processing time when a low-cost microcontroller is used. Moreover, tuning of the proportional integral (PI) controller used in the PLL is another challenge that needs to be taken into account [27]. As another approach, IRPT based algorithm does not require PLL for synchronization, however this method requires extra voltage processing operation. Moreover, this method involves active and reactive power calculation which also increases the burden on the microcontroller by increasing the processing time of the controller. Harmonic extraction based on fuzzy control [28], adaptive [29], neural-network [30], multiple adaptive feed-forward cancellation (MAFC) algorithm [31] and PLL-based algorithms [32] also provide a good performance, with a better dynamic response than Fourier, but the complexity in implementation is still a concern.

Recently harmonic extraction utilizing trigonometric orthogonal function has been proposed in literature [33]. As reported in [33], this method can bring great benefits in terms of higher processing speed for single-phase application. However, it still requires a phase lock loop which complicates the synchronization algorithm. The authors in [34] utilized the trigonometric orthogonal functions for generalized analysis of harmonic signals with non-sufficient description on application and examples. As a result of the research work in this paper, PLL can be replaced with an adaptive filter known as Self Tuning Filter (STF). STF is able to provide a clean

unitary synchronization signal irrespective of disturbances in the grid voltages [35], [36]. It is later verified in the paper, that STF can achieve the objective with fast execution time as compared to PLL.

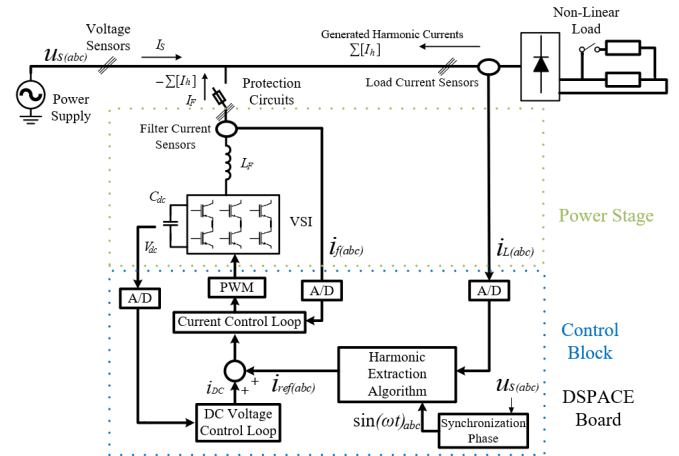


FIGURE 1: Generalized Block of Shunt APF

This paper solves the above-mentioned problems of the conventional methods via proposing a time-domain harmonics extraction approach which is the combination of trigonometric orthogonality principle (TOP) and STF technique. The proposed method (TOP) provides simpler digital implementation with lower computational burden for reference current estimation. In addition, the proposed method excludes PLL from the APF control algorithm. Instead it utilizes a simple structure of the STF for extracting fundamental component of the grid voltage, thus eliminating the complexity associated with implementation of PLL as well as isolating the APF from grid-voltage disturbances. Consequently, the proposed combination of TOP and STF forms a simple and low-computational-burden harmonic-extraction scheme which can be easily implemented in a low-cost microcontroller. Thus, a high-performance and low-cost system can be obtained.

The rest of the paper is arranged as follows: Section II discusses the operating principle of the proposed algorithm and Section III presents the generation of the synchronous phase signal. The simulation results are discussed in Section IV. The experimental results are presented in Section V and the conclusions of the paper form Section VI.

II. OPERATION PRINCIPLE OF PROPOSED ALGORITHM

The basic principle of an SAPF is shown in Fig.1, where the source current can be expressed as a combination of the load current and the filter current.

$$i_s(t) = i_L(t) + i_F(t) \quad (1)$$

The non-linear load current composes of harmonic components and a fundamental component and is given by the

Fourier series as:

$$i_L(t) = \sum_{n=1}^{\infty} I_n \sin(n\omega t + \phi_n) \quad (2)$$

$$i_L(t) = I_1 \sin(\omega t) \cos \phi_1 + I_1 \cos(\omega t) \sin \phi_1 + \sum_{n=2}^{\infty} I_n \sin(n\omega t + \phi_n) \quad (3)$$

where ω indicates the frequency ($100\pi \text{ rad/s}$) of the fundamental component. The first and second terms of (3) are active and reactive components of the fundamental load current respectively, while the third term represents the harmonics of the load current. The function of the APF is to provide the reactive content and harmonics content of the load current, such that the source only needs to supply the active component.

$$i_s(t) = I_1 \sin(\omega t) \cos \phi_1 \quad (4)$$

Hence, the source current becomes purely sinusoidal and in phase with the source voltage. The current drawn by the nonlinear load is composed of sinusoids at different multiple integrals of the fundamental frequency, and these frequency components are orthogonal to each other. Extraction of the fundamental component is obtained by eliminating the superimposed harmonics. One simple approach is to apply the trigonometric orthogonality principle, which states that the integral of the product of two orthogonal functions (y_1, y_2) is equal to zero. Mathematically, the integral of the product of two trigonometric functions in $[-\pi, \pi]$ is zero if the functions are orthogonal to each other.

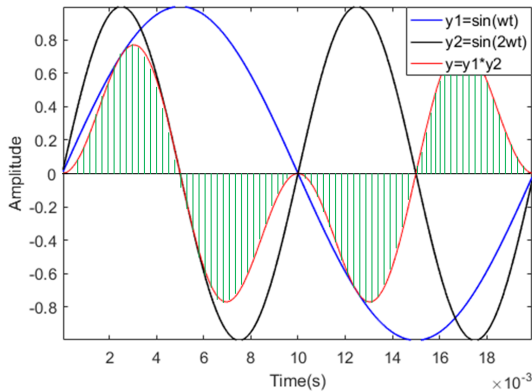


FIGURE 2: Illustration of product of trigonometric orthogonal functions

Considering two sinusoidal functions and integration of their inner product in $[-\pi, \pi]$,

$$(y_1, y_2) = \int_{-\pi}^{\pi} y_1(t)y_2(t)dt = 0 \quad (5)$$

The product above results in an odd function which is symmetric on $[-\pi, \pi]$ thus $\sin(\omega t)$ and $\cos(\omega t)$ are orthogonal to each other and their integral product results in zero.

$$\int_{-\pi}^{\pi} \sin(\omega t) \cdot \cos(\omega t) d(\omega t) = 0 \quad (6)$$

Also, $\sin(\omega t)$ is orthogonal with $\sin(k\omega t + \varphi)$ and $\cos(k\omega t)$ as long as $n \neq k$ and both are integers. Fig.2 illustrates the orthogonality principle shown by two sinusoidal functions with different frequencies. Similarly, load current is also composed of current components with different frequencies referred to as harmonic components. Therefore, by applying this principle, any component of the load current can be extracted. Usually, the active current of the fundamental component is extracted and then it is subtracted from the load current to generate the reference current. Thus the obtained reference current, which includes the harmonic and reactive current components, acts as a reference current for the APF. In order to extract the fundamental component, $i_L(t)$ is multiplied by $\sin(\omega t)$,

$$i_L(t) \cdot \sin(\omega t) = I_1 \sin(\omega t + \phi_1) \cdot \sin(\omega t) + \sum_{n=2}^{\infty} I_n \sin(n\omega t + \phi_n) \cdot \sin(\omega t) \quad (7)$$

Taking the integral of both sides,

$$\int_{-\pi}^{\pi} i_L(t) \cdot \sin(\omega t) d(\omega t) = \int_{-\pi}^{\pi} I_1 \sin(\omega t + \phi_1) \cdot \sin(\omega t) d(\omega t) + \int_{-\pi}^{\pi} \sum_{n=2}^{\infty} I_n \sin(n\omega t + \phi_n) \cdot \sin(\omega t) d(\omega t) \quad (8)$$

According to the orthogonal principle, the 2nd term of (8) on the right hand side is equal to zero, so

$$\begin{aligned} \int_{-\pi}^{\pi} i_L(t) \cdot \sin(\omega t) d(\omega t) &= \int_{-\pi}^{\pi} I_1 \sin(\omega t + \phi_1) \cdot \sin(\omega t) d(\omega t) \\ &= \frac{1}{2} I_1 \int_{-\pi}^{\pi} [\cos(\phi_1) - \cos(2k\omega t + \phi_1)] d(\omega t) \\ &= \frac{1}{2} I_1 \int_{-\pi}^{\pi} \cos(\phi_1) d(\omega t) - \frac{1}{2} I_1 \int_{-\pi}^{\pi} \cos(2k\omega t + \phi_1) d(\omega t) \end{aligned} \quad (9)$$

Again the 2nd term of (9) is also equal to zero, so

$$\begin{aligned} \int_{-\pi}^{\pi} i_L(t) \cdot \sin(\omega t) d(\omega t) &= \pi I_1 \cos \phi_1 \\ I_1 \cos \phi_1 &= \frac{1}{\pi} \int_{-\pi}^{\pi} i_L(t) \cdot \sin(\omega t) d(\omega t) \end{aligned} \quad (10)$$

Similarly multiply (3) by $\cos(\omega t)$ on both sides, and get

$$I_1 \sin \phi_1 = \frac{1}{\pi} \int_{-\pi}^{\pi} i_L(t) \cdot \cos(\omega t) d(\omega t) \quad (11)$$

Consolidate (10) and (11), we can get the fundamental component of the load current i_L ,

$$I_1 \cos \phi_1 \sin(\omega t) + I_1 \sin \phi_1 \cos(\omega t) = I_1 \sin(\omega t + \phi_1) \quad (12)$$

According to the harmonic current detection principle based on orthogonal theorem, instantaneous fundamental current can be written as;

$$i_1 = A_1 \sin(\omega t) + B_1 \cos(\omega t) \quad (13)$$

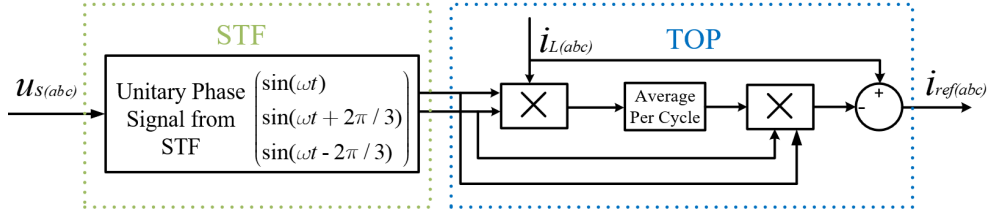


FIGURE 3: Proposed Harmonic Current Extraction Algorithm (TOP)

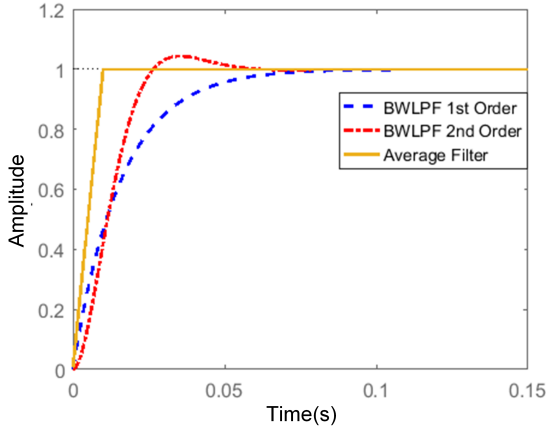


FIGURE 4: Step Response of LPF and Average Filter

where

$$A_1 = \frac{1}{\pi} \int_{-\pi}^{\pi} i_L(t) \cdot \cos(\omega t) d(\omega t) \quad (14)$$

$$B_1 = \frac{1}{\pi} \int_{-\pi}^{\pi} i_L(t) \cdot \sin(\omega t) d(\omega t) \quad (15)$$

For harmonic and reactive power compensation, the second term of (13), $B_1 \cos(\omega t)$ can be ignored, thus the fundamental component can be extracted from the load current to get the reference signal. Then this fundamental component is subtracted from load current to get the reference signal as given by

$$i_{ref(abc)} = i_{L(abc)} - i_1(abc) \quad (16)$$

Harmonic current detection method based on orthogonal theorem is shown in Fig. 3. The implementation of mean value at $[-\pi, \pi]$ is equivalent to use a low-pass filter (LPF) for eliminating AC components. However, LPF tends to make the response of the system sluggish hence an average filter is suggested. This can also be evaluated using the step response of LPF and average filter which is presented in Fig. 4. The cutoff frequency of butterworth LPF influences the dynamic speed of filter. For improved attenuation, high order and lower cutoff are desired but it comes at expense of slower transient response. The step responses of the first order LPF

($\omega_c = 10Hz$) and the second order LPF ($\omega_c = 20Hz$) are plotted alongside the step response of the average filter with window length equal to half of a fundamental cycle. It is quite evident that the average filter considerably boosts the transient of the harmonic extraction process as compared to that of butterworth LPFs.

III. SYNCHRONIZATION PHASE SIGNAL

In order to get the synchronization reference-phase signal from the source voltage, an STF based approach is adopted as shown in Fig. 5. In a practical implementation, the source voltage contains distorted components and is not purely sinusoidal or maybe unbalanced. A self-tuning filter is used to remove those unwanted components in order to get the desired clean synchronization signal. The distorted source voltage is transformed into the stationary references (alpha-beta) which include fundamental and distorted components given by

$$\begin{bmatrix} v_{s\alpha} \\ v_{s\beta} \end{bmatrix} = \begin{bmatrix} v_{s\alpha(fund.)} + v_{s\alpha(dist.)} \\ v_{s\beta(fund.)} + v_{s\beta(dist.)} \end{bmatrix} \quad (17)$$

where $v_{s\alpha(fund)}$ and $v_{s\beta(fund)}$ are the fundamental components and $v_{s\alpha(dis)}$ and $v_{s\beta(dis)}$ are the distorted components of the source voltage in the alpha-beta domain. In order to extract the fundamental component, the source voltage is passed through the STF filter and written as:

$$V_{xy} = \exp^{j\omega t} \int \exp^{-j\omega t} U_{xy} \quad (18)$$

where U_{xy} and V_{xy} are the instantaneous signals before and after integration, while ω is the angular frequency. On taking the Laplace transform of (18), we get

$$T(s) = \frac{V_{xy}(s)}{U_{xy}(s)} = \frac{s + j\omega}{s^2 + \omega^2} \quad (19)$$

By introducing an additional parameter K in $T(s)$, the transfer function will have zero phase delay and unity magnitude at the cut-off frequency $\omega = \omega_c$. Rearranging (19), we obtain the transfer function of the STF as:

$$T(s) = \frac{V_{xy}(s)}{U_{xy}(s)} = K \frac{(s + K) + j\omega}{(s + K)^2 + \omega^2} \quad (20)$$

This additional parameter now affects the filtering performance of the STF. Fig. 6 shows the filtering characteristics of the STF for different values of K . As shown in Fig. 6, the selectivity of the filter at ω_c is dependent on the parameter K . Reducing K increases the selectivity but increases the dynamics of the STF. To further illustrate this, the dynamics of the STF

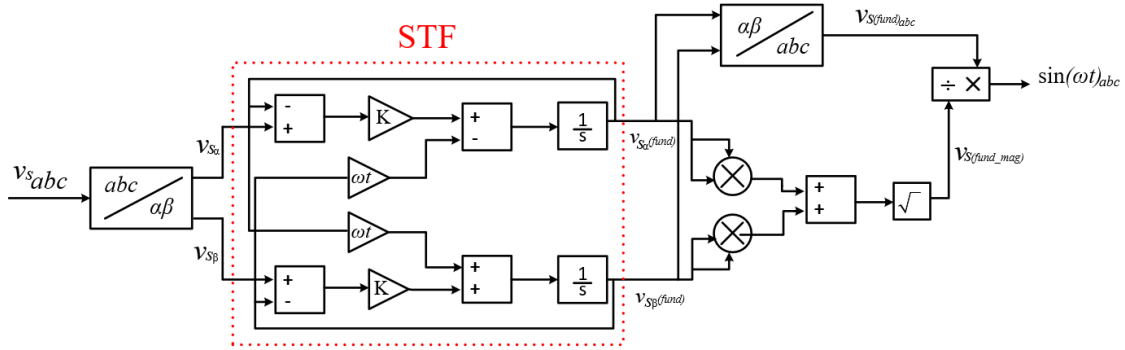
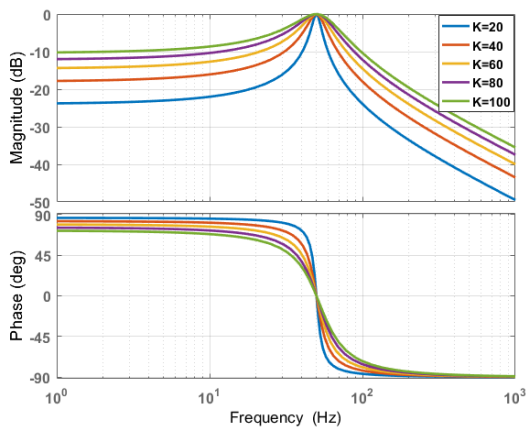


FIGURE 5: Block Diagram of synchronization phase signal

the magnitude estimation ($v_{S(fund_mag)}$) from the STF when grid voltage falls to 320V peak is shown in Fig. 7. Higher value of K results in faster dynamic response while lower value provides a sluggish behaviour in magnitude estimation, which is an integral part of unitary vector generation. Thus, K must be carefully selected to achieve a good compromise between these two features. The value of K is tuned to 100 at the fixed cut-off frequency of $f_c = 50$ Hz in order to get effective performance of the STF. If the input is replaced by $v_{s\alpha\beta}$ and the output signal by $v_{s\alpha\beta(fund)}$ and written in complex form with corresponding real and imaginary parts, (20) can be simplified as:

$$V_{s\alpha(fund.)} + jV_{s\beta(fund.)} = K \left(\frac{(s + K)}{(s + K)^2 + \omega_c^2} + \frac{j\omega_c}{(s + K)^2 + \omega_c^2} \right) (V_{s\alpha} + jV_{s\beta}) \quad (21)$$


 FIGURE 6: Bode plot of STF for various values of K

Equating real and imaginary parts, the following expressions can be obtained:

$$V_{s\alpha(fund.)} = \frac{K(s + K)}{(s + K)^2 + \omega_c^2} V_{s\alpha} - \frac{K\omega_c}{(s + K)^2 + \omega_c^2} V_{s\beta} \quad (22)$$

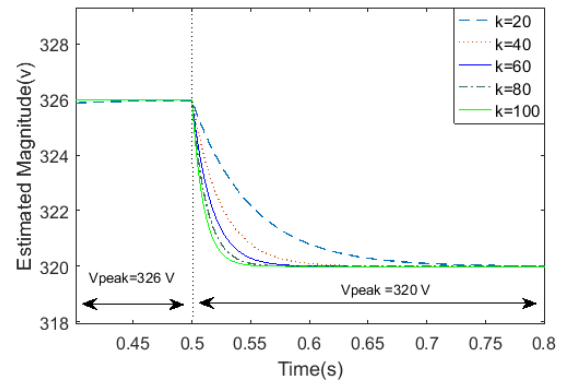


FIGURE 7: Dynamic response of magnitude estimation from STF

$$V_{s\beta(fund.)} = \frac{K(s + K)}{(s + K)^2 + \omega_c^2} V_{s\beta} + \frac{K\omega_c}{(s + K)^2 + \omega_c^2} V_{s\alpha} \quad (23)$$

Solving (22) and (23) results in

$$v_{s\alpha(fund.)} = \frac{K}{s} (v_{s\alpha} - v_{s\alpha(fund.)}) - \frac{\omega_c}{s} v_{s\beta(fund.)} \quad (24)$$

$$v_{s\beta(fund.)} = \frac{K}{s} (v_{s\beta} - v_{s\beta(fund.)}) - \frac{\omega_c}{s} v_{s\alpha(fund.)} \quad (25)$$

The generalized structure in (24) and (25) can be used to construct the STF for any two orthogonal signals formed by the $abc - \alpha\beta$ transformation. The result of (24) and (25) represents the fundamental component of the source voltage in the $\alpha\beta$ domain without distortions. The fundamental component of the source voltage in the three-phase abc domain can be obtained by the inverse Clarke transformation:

$$\begin{bmatrix} v_{sa(fund.)} \\ v_{sb(fund.)} \\ v_{sc(fund.)} \end{bmatrix} = T\alpha\beta^{-1} \begin{bmatrix} v_{s\alpha(fund.)} \\ v_{s\beta(fund.)} \end{bmatrix} \quad (26)$$

The magnitude of the fundamental component of the source voltage can be obtained by using the following calculation:

$$V_{S(fund_mag)} = \sqrt{v_{s\alpha(fund.)}^2 + v_{s\beta(fund.)}^2} \quad (27)$$

From (26) and (27), the required synchronization signal for current-harmonic extraction can be obtained as follows:

$$\begin{aligned} \sin(\omega t)_{abc} &= \frac{V_{S(fund.)_{abc}}}{V_{S(fund_mag)}} \\ &= \begin{bmatrix} \sin(\omega t) \\ \sin(\omega t - \frac{2\pi}{3}) \\ \sin(\omega t + \frac{2\pi}{3}) \end{bmatrix} \end{aligned} \quad (28)$$

The synchronizing signal is obtained by processing the source voltage directly. Hence, the obtained synchronization signal will be able to track the changes of angular position of the operating power system. This means that the synchronization signal is in phase with the source voltage. Hence, STF can be a suitable replacement for the PLL, which has been a preferred choice for APF application.

IV. SIMULATION RESULTS

TABLE 1: System Parameter used in Simulation

System Parameters	Value	Unit
Grid Voltage	220	V
Fundamental Frequency	50	Hz
DC Load Resistor - I	50	Ω
DC Load Resistor - II	50	Ω
DC Load Inductor	2	mH
DC Link Voltage	750	V
Limiting inductor	5	mH
Switching Frequency	20	kHz

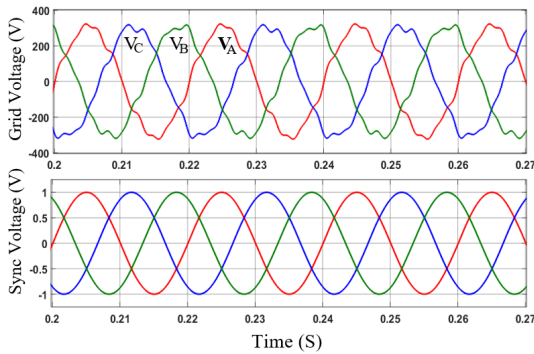


FIGURE 8: Synchronization phase signal for TOP algorithm

To validate the efficacy of the proposed approach, simulations are carried out in MATLAB Simulink environment. Firstly, the proposed synchronization signal generation (STF) and the proposed current harmonic extraction algorithm (TOP) are individually tested, and then a whole APF system including the combination of TOP and STF will be tested and analyzed. The load consists of a three-phase rectifier with a resistor and inductor on DC-side to generate the distorted current. This sort of non-linear load distorts the current with

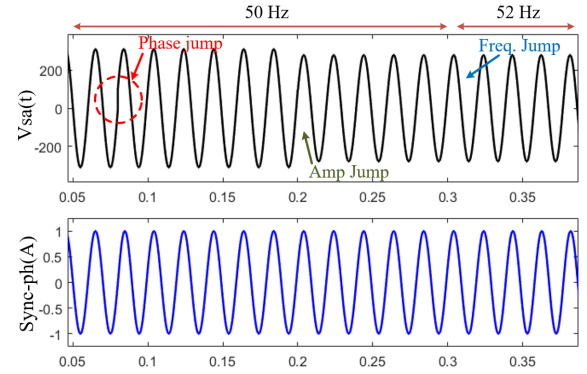


FIGURE 9: Synchronization signal generation under different grid disturbances

harmonics of order $6k \pm 1$. Table 1 provides the parameters used in the simulation study.

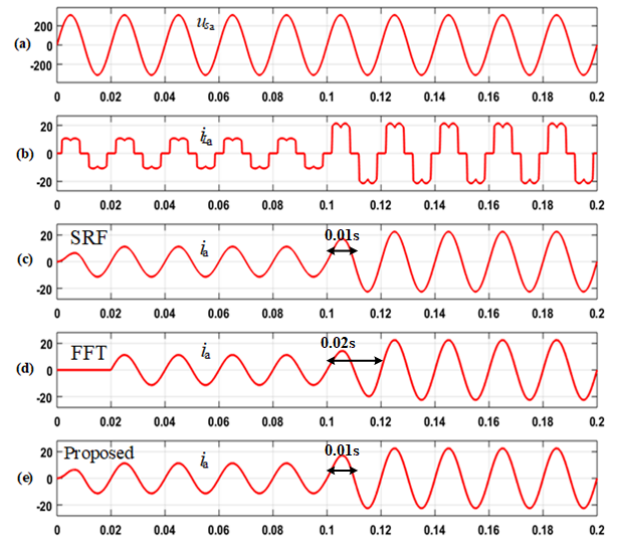


FIGURE 10: Comparison of existing algorithm along with the proposed

A. SYNCHRONIZATION SIGNAL GENERATION

The proposed TOP method requires unitary synchronization signal, which can be obtained either from a PLL or using the STF based approach as described in Section III. In PLL, the unitary sync signal is generated from the estimated phase, while in STF based method, the unitary signal is obtained by normalizing the filtered signal with the grid voltage magnitude. Both approaches provide distortion free synchronization signal with the THD below 1%. However, STF based method has advantage over the PLL in terms of implementation and resource consumption which is verified in experimental section. Fig. 8 represents the synchronization phase signal generated using the STF-based procedure in distorted grid condition. It can be seen from Fig. 8 that, even in abnormal grid scenario the obtained synchronization phase

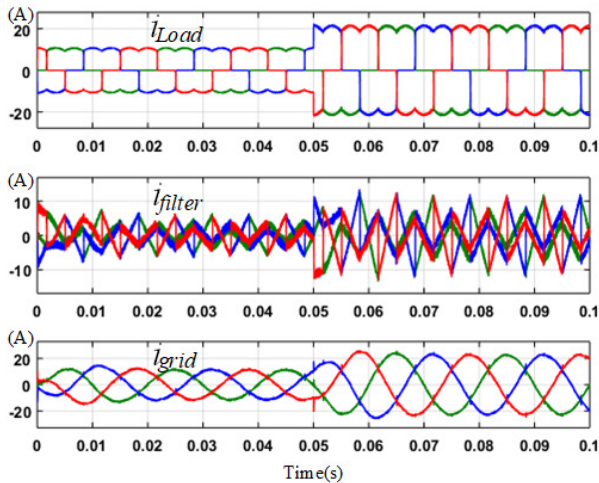


FIGURE 11: Overall compensation result of three-phase APF with TOP algorithm

signal contains a pure fundamental component (THD = 0.1%) of the source voltage. Another test is conducted for evaluating STF performance, where the grid voltage undergoes phase jump (+30°) at $t = 0.08s$, amplitude change (283V) at $t = 0.2s$ and frequency jump (2Hz) at $t = 0.32s$. In all these three disturbances, the STF is able to generate accurate unitary synchronization signal. This is illustrated through simulation results shown in Fig. 9. This synchronization signal is used as a phase reference for the proposed current harmonic-extraction algorithm (TOP) which eliminates the use of a PLL. The operation of STF only relies on grid voltage and has no dependency on the operation of TOP or APF system.

TABLE 2: Comparison of occupied resources

Harmonic Detection Algorithm	Adder	Multiplier	Array
<i>DQ</i>	13	18	2
<i>Fourier</i>	17	25	6
<i>TOP</i>	8	13	3

B. STEADY-STATE AND DYNAMIC ANALYSIS

In this section, the dynamic and the steady-state response of the proposed TOP method in generating the fundamental component of the load current is analyzed and compared with the two well-known SRF and Fourier-transform techniques. To check the transient response, an additional switch is employed which is triggered at 0.1 s to provide a step change to the load. Fig. 10 (a) and Fig. 10 (b) represent the grid voltage, which is sinusoidal, and the load current, which is distorted and contains harmonics. To make a fair comparison, an Average Filter, as explained in Section II, with window size of 20 ms is used for both TOP and SRF methods. This filter can eliminate the effect of the DC component in the measured current, which translates to sinusoidal at 50 Hz. As shown in Fig. 10 (d), Fourier-transform based method exhibits the transient response of at

least one complete fundamental cycle. Fig. 10 (c) and 10 (e) represent the fundamental component extraction by the SRF and the proposed algorithm respectively. The SRF and the proposed method show the same steady-state and dynamic performance, which takes only half a cycle to settle down during the load variation.

From the simulation results in Fig. 10, although the proposed TOP and SRF methods exhibit the same dynamic response during the load variation, from an implementation point of view, the proposed method is superior due to its less number of calculations involved. This has direct impact on processing time of microcontrollers and is beneficial in industrial applications where low-cost microcontrollers are preferable. Table 2 presents the number of mathematical calculations involved in the three tested methods. Among these, Fourier transform requires a large number of mathematical calculations. Additionally, Fourier requires large memory compared to any other approach. It can be seen that TOP provides an efficient implementation and can be considered as a suitable alternative for a low-cost implementation.

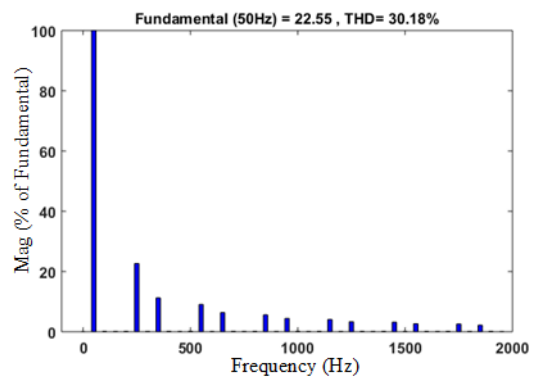


FIGURE 12: FFT before compensation

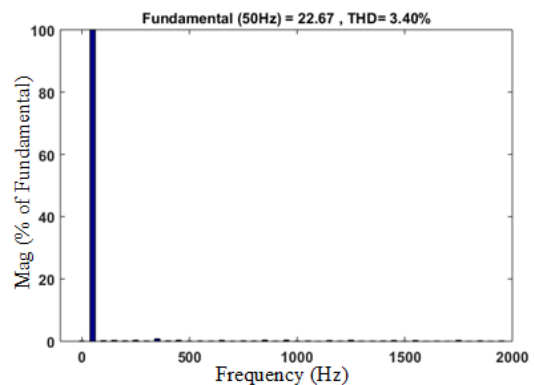


FIGURE 13: FFT after compensation

C. COMPENSATION PERFORMANCE ANALYSIS

In this section, the operation of the whole APF system, including the proposed TOP method for harmonics extraction

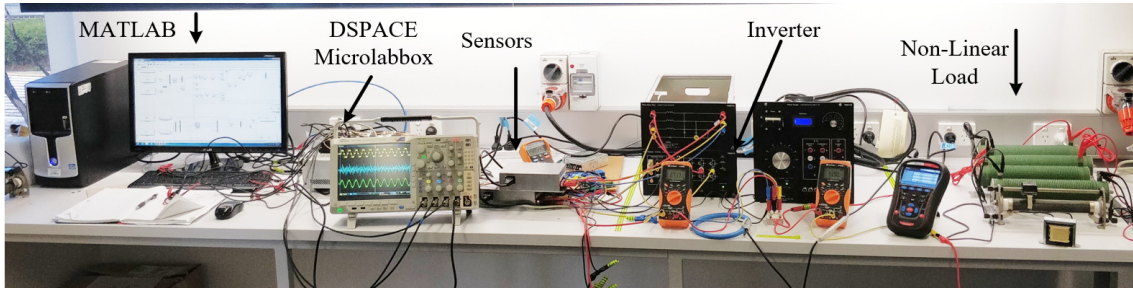


FIGURE 14: Experimental Setup in Laboratory

and STF for synchronization, is tested and analyzed. Fig. 11 represents the compensation performance of a three-phase APF during the steady-state and at load variations. It can be seen that during a load change, the system using the proposed approach requires half of the fundamental cycle to reach the steady-state mode, which meets the simulation results in Fig. 10 (d). The THD of source current before and after compensation are depicted in Fig. 12 and Fig. 13 respectively. THD is below 5% after compensation, thus fulfilling the restriction set by IEEE-standard 519-2014. This verifies the successful operation of the whole APF system including both proposed TOP and STF for synchronization.

TABLE 3: System Parameters used in Experiment

System Parameter	Value	Unit
Grid Voltage	50	V
Fundamental Frequency	50	Hz
DC Link Voltage	240	V
Output Filter	3	mH
Switching Frequency	20	kHz

V. EXPERIMENT RESULTS

The aim of the experimental results in this section is to validate the simulation results as well as verifying the lower complexity and processing time of the proposed approach than the conventional methods. In this regard, the focus has been on the harmonic current extraction rather than the operation of whole APF system. A hardware prototype is developed in the laboratory to validate the proposed current harmonic-extraction algorithm as well as compare it with other conventional approaches. The configuration of the hardware setup is the same as shown in Fig. 1, and the overall laboratory setup is shown in Fig. 14. A three-phase variable AC source is used as a supply voltage connected with the APF and the non-linear load. The nonlinear load is a three-phase uncontrolled rectifier. A dSPACE Microlabbox 1102 is used for implementing the proposed algorithm and for controlling the APF. The main parameters used in the experiment are given in the Table 4.

The proposed TOP method is a PLL less system, and its required synchronization phase signals are obtained from the STF based algorithm. The synchronization phase signals, which are shown in Fig. 15, are purely sinusoidal and contain

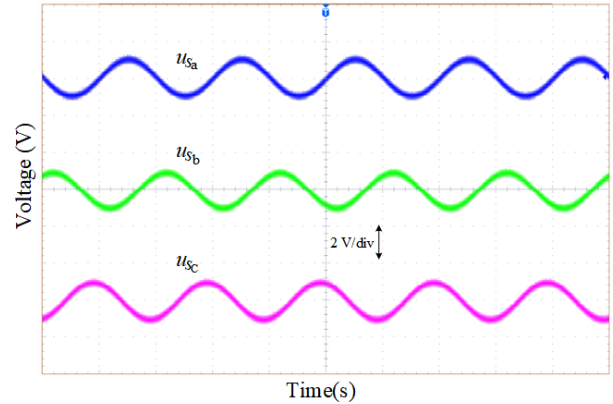


FIGURE 15: Synchronization phase signal

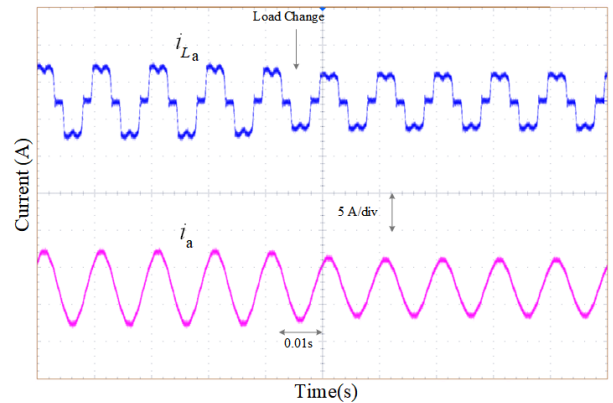


FIGURE 16: Fundamental current extraction using TOP

phase information of the grid voltage. The experimental result in Fig. 15 is consistent with the simulation result in Fig. 8. The STF method is as effective as PLL but with reduced computation burden and complexity. Comparing the execution times of a standard PLL and STF (measured and reported by dSPACE 1102), the STF requires only $0.34\mu\text{s}$ which is 10 times smaller than $3.6\mu\text{s}$ required by the standard PLL. A similar execution times will also be noted if other microcontrollers are used in place of dSPACE because of lower computational requirement from the proposed method.

Fig. 16 illustrates the extracted fundamental component

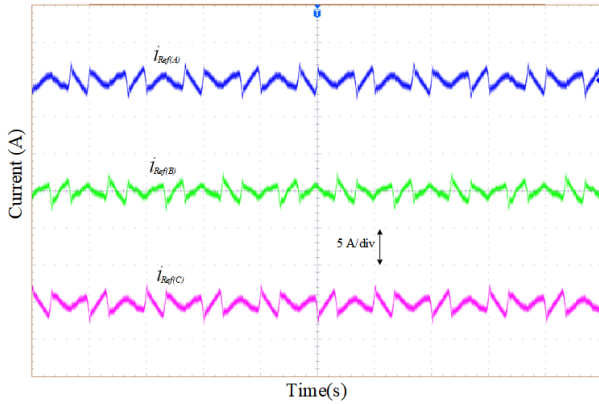


FIGURE 17: Current Harmonic Reference Signal

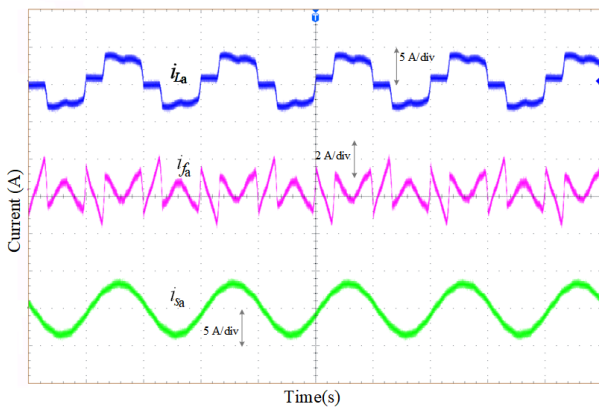


FIGURE 18: APF Compensation Performance with TOP

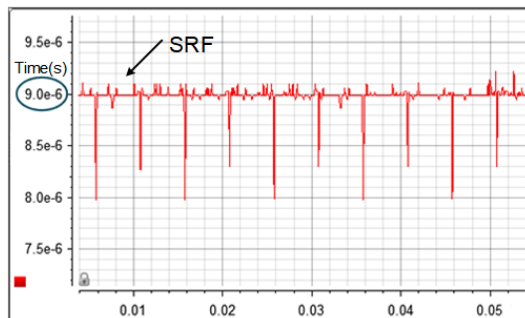


FIGURE 19: Execution Time of SRF Algorithm

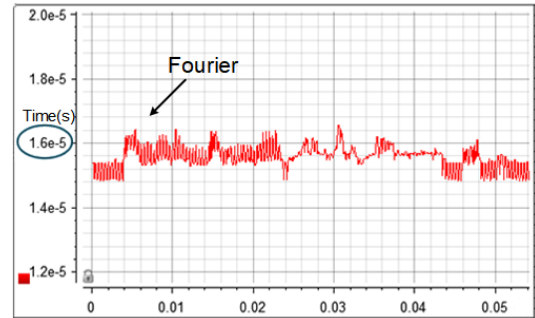


FIGURE 20: Execution Time of Fourier Algorithm

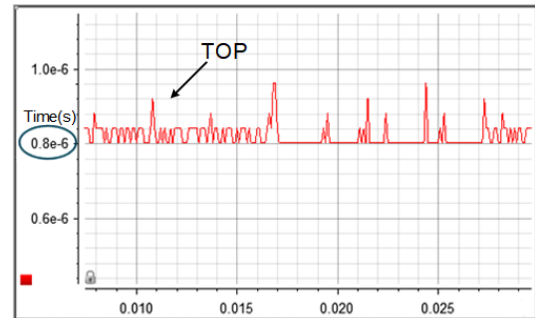


FIGURE 21: Execution Time of TOP Algorithm

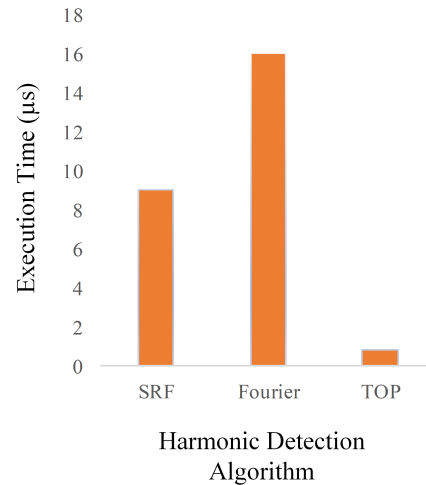


FIGURE 22: Comparison of Execution Time of Harmonic-Extraction Algorithm

of the load current using the proposed TOP algorithm. As already shown in Fig. 10 and experimentally verified in Fig. 16, the proposed TOP method can extract the fundamental component with minimum THD and within half cycle during transient same as SRF method. The corresponding harmonic reference currents generated by TOP are shown in Fig. 17 which will be used as reference for the controller of APF.

The compensation performance of the APF, utilizing the proposed structure of TOP and STF, is shown in Fig. 18 where the load current, the harmonics current and the source current are presented. The sinusoidal nature of the source

current and with the THD below 5% verifies the accuracy of the proposed TOP-STF based harmonic extraction method.

So far, the experimental results have shown the effectiveness of the proposed method, which is equivalent to the conventional SRF method. However, as mentioned throughout the paper and shown in Table II, the proposed approach exhibits a lower computational burden than SRF. This advantage is verified in this section by experimentally observing the execution time of each algorithm in the control desk of dSPACE 1102 presented in Fig. 19, Fig. 20 and Fig. 21.

TABLE 4: Summarized comparison of the proposed methods with conventional methods

Method	Transient Duration	Steady State Accuracy	Implementation Complexity
SRF	Half cycle	Good	Medium
FFT	One cycle	Good	High
Proposed	Half cycle	Good	Low

As can be seen, the proposed TOP-STF method requires 0.8 μ s execution time, while Fourier-transform method exhibits 16 μ s and SRF shows 9 μ s. The execution times of the three algorithms are plotted and compared in Fig. 22. From Fig. 22, it can be concluded that the proposed method takes the minimum time for execution which is highly beneficial, especially if the sampling window time is less, for instance, with high sampling frequency. The lower processing times gives enough remaining window time for other control tasks such as the execution of current and voltage control loops.

Performance evaluations of the proposed method compared with the conventional SRF and FFT are summarized in Table 4.

VI. CONCLUSION

This paper proposes a new harmonic extraction approach which uses TOP principle. The replacement for a PLL, as used by the conventional methods, was realized with a simple structure comprised of an STF for synchronization. As a result, the proposed TOP method exhibits lower complexity and computational burden. The underlying principle of the TOP and STF are discussed in detail and the performance of the proposed method is compared with conventional techniques. The simulation, analysis and experimental results verify the superiority of the proposed method in terms of its accuracy, dynamics and implementation. The TOP method is at least 10 times faster than the SRF and 20 times than the fourier based method. The proposed harmonics extraction approach would be an interesting alternative for industrial used APFs where low-cost microcontrollers are preferable. The future research will focus on including the selective harmonic compensation capability of the proposed method.

REFERENCES

- [1] S. Bosch, J. Staiger, and H. Steinhart, "Predictive current control for an active power filter with lcl-filter," *IEEE Transactions on Industrial Electronics*, vol. 65, no. 6, pp. 4943–4952, 2018.
- [2] J. P. Thomas, P. S. Revuelta, A. P. Vallés, and S. P. Litrán, "Practical evaluation of unbalance and harmonic distortion in power conditioning," *Electric Power Systems Research*, vol. 141, pp. 487–499, 2016.
- [3] Q. Liu, Y. Li, S. Hu, and L. Luo, "A transformer integrated filtering system for power quality improvement of industrial dc supply system," *IEEE Transactions on Industrial Electronics*, 2019.
- [4] Q. Liu, Y. Li, L. Luo, Y. Peng, and Y. Cao, "Power quality management of pv power plant with transformer integrated filtering method," *IEEE Transactions on Power Delivery*, vol. 34, no. 3, pp. 941–949, 2018.
- [5] J. C. Alfonso-Gil, E. Pérez, C. Arino, and H. Beltran, "Optimization algorithm for selective compensation in a shunt active power filter," *IEEE Transactions on Industrial Electronics*, vol. 62, no. 6, pp. 3351–3361, 2015.
- [6] A. Eid, M. Abdel-Salam, H. El-Kishky, and T. El-Mohandes, "Active power filters for harmonic cancellation in conventional and advanced aircraft electric power systems," *Electric Power Systems Research*, vol. 79, no. 1, pp. 80–88, 2009.
- [7] M. Kashif, M. Hossain, F. Zhuo, and S. Gautam, "Design and implementation of a three-level active power filter for harmonic and reactive power compensation," *Electric Power Systems Research*, vol. 165, pp. 144–156, 2018.
- [8] W. U. K. Tareen and S. Mekhief, "Three-phase transformerless shunt active power filter with reduced switch count for harmonic compensation in grid-connected applications," *IEEE Transactions on Power Electronics*, vol. 33, no. 6, pp. 4868–4881, 2018.
- [9] R. Kumar and H. O. Bansal, "Hardware in the loop implementation of wavelet based strategy in shunt active power filter to mitigate power quality issues," *Electric Power Systems Research*, vol. 169, pp. 92–104, 2019.
- [10] D. Bernet and M. Hiller, "Grid-connected medium-voltage converters with parallel voltage-source active filters," *IET Electric Power Applications*, 2019.
- [11] L. Merabet, S. Saad, D. O. Abdeslam, and A. Omeiri, "A comparative study of harmonic currents extraction by simulation and implementation," *International Journal of Electrical Power & Energy Systems*, vol. 53, pp. 507–514, 2013.
- [12] M. Kashif, M. Hossain, F. Zhuo, S. Shi, and J. L. Soon, "An advanced harmonic extraction technique applied to a three-phase three-level active power filter," in *Future Energy Electronics Conference and ECCE Asia (IFEEC 2017-ECCE Asia)*, 2017 IEEE 3rd International. IEEE, 2017, pp. 364–369.
- [13] L. Asiminoel, F. Blaabjerg, and S. Hansen, "Detection is key-harmonic detection methods for active power filter applications," *IEEE Industry Applications Magazine*, vol. 13, no. 4, pp. 22–33, 2007.
- [14] A. Boussaid, A. L. Nemmour, L. Louze, and A. Khezzer, "A novel strategy for shunt active filter control," *Electric Power Systems Research*, vol. 123, pp. 154–163, 2015.
- [15] S. Gautam, D. D.-C. Lu, Y. Lu, and W. Xiao, "Fast identification of active and reactive current component for single phase grid interconnection," in *2017 20th International Conference on Electrical Machines and Systems (ICEMS)*. IEEE, 2017, pp. 1–6.
- [16] T. Green and J. Marks, "Control techniques for active power filters," *IEE Proceedings-Electric Power Applications*, vol. 152, no. 2, pp. 369–381, 2005.
- [17] R. S. Herrera, P. Salmerón, and H. Kim, "Instantaneous reactive power theory applied to active power filter compensation: Different approaches, assessment, and experimental results," *IEEE Transactions on Industrial Electronics*, vol. 55, no. 1, pp. 184–196, 2008.
- [18] L. A. Moran, J. W. Dixon, and R. R. Wallace, "A three-phase active power filter operating with fixed switching frequency for reactive power and current harmonic compensation," *IEEE Transactions on Industrial Electronics*, vol. 42, no. 4, pp. 402–408, 1995.
- [19] F. A. Neves, H. E. de Souza, F. Bradaschia, M. C. Cavalcanti, M. Rizo, and F. J. Rodriguez, "A space-vector discrete fourier transform for unbalanced and distorted three-phase signals," *IEEE Transactions on Industrial Electronics*, vol. 57, no. 8, pp. 2858–2867, 2010.
- [20] F. A. Neves, H. E. de Souza, M. C. Cavalcanti, F. Bradaschia, and E. J. Bueno, "Digital filters for fast harmonic sequence component separation of unbalanced and distorted three-phase signals," *IEEE Transactions on Industrial Electronics*, vol. 59, no. 10, pp. 3847–3859, 2012.
- [21] H. Liu, H. Hu, H. Chen, L. Zhang, and Y. Xing, "Fast and flexible selective harmonic extraction methods based on the generalized discrete fourier transform," *IEEE Transactions on Power Electronics*, vol. 33, no. 4, pp. 3484–3496, 2018.
- [22] F. Z. Peng and J.-S. Lai, "Generalized instantaneous reactive power theory for three-phase power systems," *IEEE transactions on instrumentation and measurement*, vol. 45, no. 1, pp. 293–297, 1996.
- [23] S. Wamane, J. Baviskar, and S. Wagh, "A comparative study on compensating current generation algorithms for shunt active filter under non-linear load conditions," *Int. J. Sci. Res. Publ.*, vol. 3, no. 6, pp. 1–6, 2013.
- [24] S. Gautam, P. Yunqing, Y. Kafle, M. Kashif, and S. U. Hasan, "Evaluation of fundamental dq synchronous reference frame harmonic detection method for single phase shunt active power filter," *International Journal of Power Electronics and Drive Systems*, vol. 4, no. 1, p. 112, 2014.
- [25] S. Golestan, J. M. Guerrero, A. Vidal, A. G. Yepes, and J. Doval-Gandoy, "PII with maf-based prefiltering stage: small-signal modeling and performance enhancement," *IEEE Transactions on Power Electronics*, vol. 31, no. 6, pp. 4013–4019, 2016.

- [26] S. Gautam, Y. Lu, W. Hassan, W. Xiao, and D. D.-C. Lu, "Single phase ntd pll for fast dynamic response and operational robustness under abnormal grid condition," *Electric Power Systems Research*, vol. 180, p. 106156, 2020.
- [27] P. Rodríguez, J. Pou, J. Bergas, J. I. Candela, R. P. Burgos, and D. Boroyevich, "Decoupled double synchronous reference frame pll for power converters control," *IEEE Transactions on Power Electronics*, vol. 22, no. 2, pp. 584–592, 2007.
- [28] L. Saribulut, A. Teke, and M. Tümay, "Artificial neural network-based discrete-fuzzy logic controlled active power filter," *IET Power Electronics*, vol. 7, no. 6, pp. 1536–1546, 2014.
- [29] V. Blasko, "A novel method for selective harmonic elimination in power electronic equipment," *IEEE transactions on Power Electronics*, vol. 22, no. 1, pp. 223–228, 2007.
- [30] H. C. Lin, "Intelligent neural network-based fast power system harmonic detection," *IEEE Transactions on Industrial Electronics*, vol. 54, no. 1, pp. 43–52, 2007.
- [31] S. Leng, W. Liu, I.-Y. Chung, and D. Cartes, "Active power filter for three-phase current harmonic cancellation and reactive power compensation," in *2009 American Control Conference*. IEEE, 2009, pp. 2140–2147.
- [32] Y. F. Wang and Y. W. Li, "Three-phase cascaded delayed signal cancellation pll for fast selective harmonic detection," *IEEE Transactions on industrial electronics*, vol. 60, no. 4, pp. 1452–1463, 2013.
- [33] H. Yi, F. Zhuo, F. Wang, Y. Li, and Z. Wang, "A single-phase harmonics extraction algorithm based on the principle of trigonometric orthogonal functions," *Journal of Power Electronics*, vol. 17, no. 1, pp. 253–261, 2017.
- [34] R. Wang, Y. Zhang, and J. Guo, "Power harmonic analysis based on orthogonal trigonometric functions family," in *CICED 2010 Proceedings*. IEEE, 2010, pp. 1–7.
- [35] P. Chittora, A. Singh, and M. Singh, "Application of self tuning filter for power quality improvement in three-phase-three-wire distorted grid system," in *2017 7th International Conference on Power Systems (ICPS)*. IEEE, 2017, pp. 313–318.
- [36] S. Swain and B. Subudhi, "A new grid synchronisation scheme for a three-phase pv system using self-tuning filtering approach," *IET Generation, Transmission & Distribution*, vol. 11, no. 14, pp. 3557–3567, 2017.



MUHAMMAD KASHIF (S'16) received a B.Sc degree from the University of Engineering and Technology, Peshawar, Pakistan in 2008 and the MSc degree from Xi'an Jiaotong University (XJTU), China in 2013 in Telecommunication Engineering and Electrical Engineering respectively. While, in XJTU, he was associated with Power Electronics and Renewable Energy Research Centre, as a graduate research student. He is currently working towards his Ph.D. degree in Electronics Engineering (Power Electronics) at Macquarie University, Sydney, Australia since 2016. His research interest includes power quality-related issues and their solutions, active power filters, renewable energy system, energy conversion and control of grid interfaced power converters.



M. JAHANGIR HOSSAIN (M'10-SM'13) received the B.Sc. and M.Sc. Eng. degrees from Rajshahi University of Engineering and Technology (RUET), Bangladesh, in 2001 and 2005, respectively, and the Ph.D. degree from the University of New South Wales in 2010, Australia, all in electrical and electronic engineering. He is currently an Associate Professor with the School of Electrical and Data Engineering, University of Technology, Sydney, Australia. Before joining there, he served as an Associate Professor in the School of Engineering, Macquarie University, Senior Lecture and a Lecturer in the Griffith School of Engineering, Griffith University, Australia for five years and as a Research Fellow in the School of Information Technology and Electrical Engineering, University of Queensland, Brisbane, Australia. His research interests include renewable energy integration and stabilization, voltage stability, micro grids and smart grids, robust control, electric vehicles, building energy management systems, and energy storage systems.



EDSTAN FERNANDEZ (S'17) received the M.Tech. degree from the Vellore Institute of Technology, Vellore, India in Sensor System Technology. Currently, he is pursuing the Ph.D. degree in electrical engineering at Macquarie University, Sydney, Australia. His research interests are demand side management, power system automation, optimization and control of energy management systems in smart-grids and game theoretic approach to EMS.



SEYEDFOAD TAGHIZADEH received his Ph.D. degree in Electrical Engineering from the Macquarie University, Australia, in 2018. He is currently working as a Research Fellow in the School of Engineering, Macquarie University, Australia. His research interests include electric vehicle chargers, control systems, renewable energy integration, power quality, and energy storage systems.



VIVEK SHARMA (S'17) received the B.Eng and M.Eng degree in electrical engineering from India. He is currently working towards the Ph.D. degree in electrical engineering at Macquarie University, Sydney, Australia. His research interests include fault diagnosis and fault-tolerant control of electric motor drives.



S. M. NAWAZISH ALI (S'17) received the B.Sc. and M.Sc. degrees in electrical engineering from University of Engineering and Technology (UET), Lahore, Pakistan, in 2013 and 2016, respectively. He is currently working towards his Ph.D. degree in electrical engineering at Macquarie University, Sydney, Australia. His research interests include control design and analysis of thermal phenomenon in traction motors of electric vehicles.



USAMA BIN IRSHAD (S'18) received a B.Sc. degree in electrical (power) engineering from COMSATS institute of information technology, Pakistan, in 2012 and an M.Sc. degree in electrical engineering from King Fahd University of Petroleum and Minerals, Saudi Arabia. Currently, he is pursuing his Ph.D. degree in science and engineering from Macquarie University, Australia. His research interests are mainly in power system modeling, optimization and control, integration of renewable energy sources, electric vehicles, energy management, smart grid, energy storage systems, power system analysis and intelligent control systems.

...